Canonical cell model of Cadmium-based icosahedral alloys

M. Mihalkovič
Institute of Physics, Slovak Academy of Sciences, 84511 Bratislava, Slovakia

M. Widom
Department of Physics, Carnegie Mellon University
Pittsburgh, PA 15213
(Dated: May 15, 2005)

Cadmium-based quasicrystals (Cd-Ca and Cd-Yb) were the first binary alloys discovered to form thermodynamically stable quasicrystals. As a binary alloy, and with a strong size difference between atomic species, they are ideal system for structural and thermodynamic analysis. Observed quasicrystal approximants with crystallographically determined structures can be interpreted as decorations of Henley's canonical cells. We use first-principles total energy calculations to resolve details of the most favorable decorations.

PACS numbers:

I. INTRODUCTION

Thermodynamically stable binary icosahedral quasicrystals occur in the alloy systems $Cd_{5.7}Yb$ and $Cd_{5.7}Ca$ [1–3]. Since their discovery numerous attempts have been made to model their structure. Efforts that rely on "atomic surfaces" and higher dimensional space suffer difficulty since certain atomic positions appear to be displaced far from any simply represented position. Atomic surface representations also average over disorder phenomena in a manner that may hide important details of the structure.

Assuming that the fundamental building motif of the structure is the large $Ca_{12}Cd_{54}$ atom cluster (see Fig. 1) observed in "1/1" approximant, a phase that is stable over a range of Cd-rich systems [4], an alternative approach to modelling the quasicrystal structure is to specify how the clusters arrange to fill space quasiperiodically, and also fill some empty regions with "glue" atoms. We simultaneously resolve both these issues within the cluster model by decorating canonical cells [5, 6] with clusters and glue atoms, then filling space using canonical cell tilings. First-principles total energy calculations suggest our proposed structures are plausible.

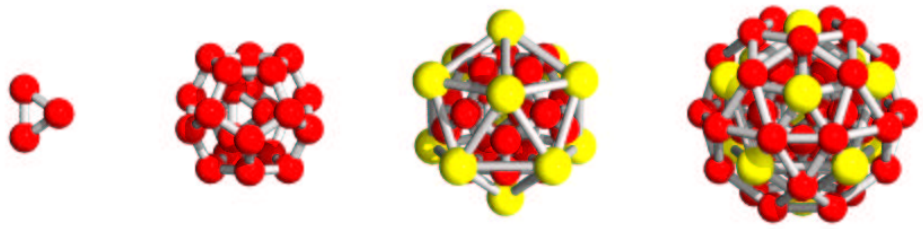

FIG. 1: Adding shells to Ca12Cd54 cluster. Left to right: (s1) Cd_4 tetrahedron (atom at back right hidden from view); (s2) Cd_{20} dodecahedron; (s3) Ca_{12} icosahedron; (s4) Cd_{30} icosidodecahedron.

Cadmium-based quasicrystals create interest both because of their unusual structure and because they occur as binary alloys. Binary alloy systems can be simpler to study, both experiemntally and theoretically, than the ternary alloy systems in which previously known thermodynamically stable quasicrystals occur. One advantage of a binary alloy is the presence of just a single composition variable to control, as opposed to two independent compositions in a ternary. Another advantage, from a theoretical perspective, is the strong size constrast between the large Ca or Yb atoms (nominal diameters 3.95 and 3.88 Å) and the relatively small Cd atoms (nominal diameter 2.98 Å). These elements also exhibit strong differences in electronegativity and other chemical properties. As a result, chemical substitution resulting in mixed site occupancy unlikely. In contrast, at least one pair of elements substitute easily for each other in the stable ternary quasicrystals.

Our approach uses the crystallographically known structures of quasicrystal approximants to validate the basic cluster structure and to identify likely positions of "glue atoms" in the space between clusters. We use first-principles total energy calculations to optimize our models and resolve details not available from the known approximants, either

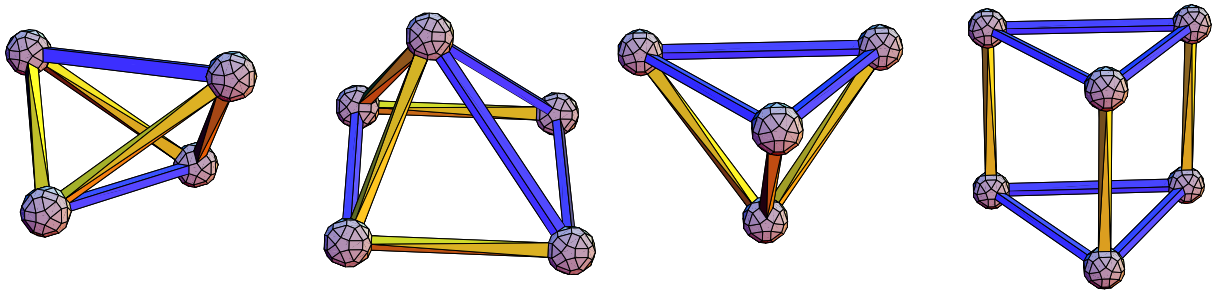

FIG. 2: Canonical Cells [5] (left to right, A, B, C, D) illustrated as if constructed from ZomeTools. Icosahedral balls occupy vertices. Blue and yellow edges lie along 2-fold and 3-fold directions.

because of intrinsic structural disorder in the materials or because of the limited number of known structures that can be used as examples.

II. CANONICAL CELLS

Our Ca-Cd decoration models utilize tilings of "canonical cells" [5]. Space is divided into 4 kinds of cells, denoted A, B, C and D (see Fig. 2). Cell vertices are occupied by nonoverlapping icosahedral clusters linked along 2-fold and 3-fold icosahedral directions, which are called b and c bonds. The A-cell is a BCC tetrahedron, the B-cell is a rectangular pyramid, the C-cell is triangular tetrahedron and the D-cell is a trigonal prism. Cell faces are of three types: X (isosceles triangle with 1 b and 2 c edges); Y (equilateral triangle with 3 b edges); Z (rectangle with 2 b and 2 c edges). Packing constraints guarantee that B and C cells occur in equal numbers.

Canonical cell tilings can be decomposed into tilings by oblate (OR) and prolate (PR) rhombohedra whose edges run along 5-fold directions. Each cell node becomes a vertex in the rhombohedral tiling with edges in all twelve directions. Each 2-fold b bond becomes a rhombic dodecahedron (RD, which decomposes into 2 OR and 2 PR). Each 3-fold c bond becomes a PR. A PR pierces through each Y-face and also an OR lies on each Z-face. The D cell actually contains four interior PR's, the one piercing its Y-face, plus three more associated with the three interior (fake) c-bonds.

In the following we consider the energetics of several canonical cell tilings. Table I lists some of their properties.

TABLE I: Canonical cell tilings considered in this work. Pearson symbol of tiling, name of known compound, space group, numbers of objects per unit cell, first-principles energy, total number of atoms N_{tot} and the fraction of "glue" atoms n_{glue}.

Name.Pearson	Compound	Symmetry	Nodes	A	B	C	D	ΔE	N_{tot}	n_{glue}
A.cI2	$CaCd_6$	$Im\bar{3}$	2	12	0	0	0	stable	168	0.21
BC.hR1		$R\bar{3}m$	1	0	2	2	0	2.8	94	0.30
D.hP1		$P\bar{3}m$	1	0	0	0	1	6.7	126	0.48
ABC.cP8	$Ca_{13}Cd_{76}$	$Pa\bar{3}$	8	24	8	8	0	2.9	712	0.26
ABC.mP2		$P2$	2	6	2	2	0	6.4	178	0.26
ABC.mP4		$P2_1/c$	4	12	4	4	0	6.6	356	0.26
ABCD.hR3		$R3m$	3	6	3	3	1	2.6	288	0.31
ABCD.mP4		$P2/m$	4	6	4	4	2	6.9	398	0.34

Two of the tilings correspond to known Ca-Cd structures. The $CaCd_6$ structure, also known as the 1/1 cubic approximant, is the pure A-cell tiling A.cI2. The precise structures remain controversial with Pearson type given variously as cI160, cI176, cI184 and cI232 [4, 7–11] as a result of uncertainty regarding the proper orientations of the Cd_4 cluster center tetrahedra. In fact, there appears to be a low temperature (around T=100K) order-disorder phase transition [11–13] in which these tetrahedra lock into specific relative orientations. Our calculations [14] confirm that ordering into particular cluster orientations can lower the energy slightly but that at elevated temperatures this degree

of freedom should indeed be disordered, so the structure is body-centered cubic, with two basic $Ca_{12}Cd_{54}$ clusters plus 36 Cadmium glue atoms per simple cubic cell.

The BCC structure tiles space with canonical A cells, with a cluster center at each A-cell vertex. Each simple cubic cell contains 12 A-cells. The 1/1 approximant structure implies a unique decoration of the A-cell, same for the cluster center tetrahedra. The other solved approximant structure [15] is the 2/1 cubic approximant, $Ca_{13}Cd_{76}$. We recognize this as the ABC.cP8 tiling, containing 24A, 8B and 8C cells. The decoration implied for the A-cell agrees precisely with that obtained from the 1/1 approximant. We bind all "glue" atoms that are not inferred by A–cell decoration motif to Y and Z faces of the CCT. A more detailed description is given in Sec. IV.

Mapping the aforementioned known approximant structures on the CCT objects specifies complete decorations for A, B and C cells (we actually use Y–face object to capture all glue atoms inside B and C cells). Thus the only remaining significant gap in the model is the decoration of the D–cell. Since there are no experimental clues as to what should the optimal decoration there be, we combine intuitive approach based on the rather surprising analogy with i-AlMnSi quasicrystal structure with ab–initio total energy calculations to resolve this missing part of the structure (Sec. IV).

The structure Ca_2Cd_7.hP68 is based on trigonal prisms, whose triangular faces are Y-faces, but their rectangular faces are not Z-faces, so this structure is not a CCT, and should not be considered a proper approximant. The clusters based at trigonal prism vertices are imperfect basic clusters, and instead of being centered by Cd_4 tetrahedra, they are centered by Cd_3 triangles.

III. TOTAL ENERGY CALCULATIONS

We carry out *ab-initio* calculations using the plane-wave program VASP [16, 17] which yields reasonably accurate total energies. This approach uses ultrasoft pseudopotentials [18, 19] and PAW potentials [20] to represent the effective interaction of valence electrons with ionic cores, and solves the many-body quantum mechanical band structure of these electrons using electronic density functional theory. We choose to model Cd-Ca rather than Cd-Yb because the alkali earth element Ca is easier to treat from first principles than the rare earth element Yb.

First, we use VASP to reproduce the sequence of low-temperature stable phases in the established Ca-Cd binary phase diagram [21]. To do this we calculate the cohesive energy for each known structure, and several hypothetical ones. Each structure is fully relaxed in both unit cell parameters and atomic coordinates. All energies are converged to an accuracy of 1 meV/atom or better by increasing the k-point mesh density. These calculations use PAW potentials in the generalized gradient approximation and a constant plane-wave energy cutoff of 274 eV.

For largest of our approximant structures (ABC.cP8 tiling, 712 atoms in cubic cell), the relaxations presented a formidable computational task. The Γ–point–only calculation required ∼16Gb memory, and one ionic step took ∼12–20 hours CPU time on 8 Opteron processors. The final energy reported in the Tab. I refers to a structure pre-relaxed using EAM potentials [22], and final VASP calculation at K =(1/4,1/4,1/4) to avoid any spurious effect arising from the highly symmetric Γ–point calculation.

Subtracting each cohesive energy from the tie-line joining the pure elements in their ground states yields enthalpies of formation ΔH_{for} (at T=0K). Enthalpies of all known and many hypothetical Ca-Cd structures are plotted in Fig. 3. We label each structure with its name followed by its Pearson symbol.

Agreement between our calculation and the established phase diagram requires that all known low temperature structures lie on the convex hull of enthalpy versus composition. Additionally, all hypothetical structures must lie above the convex hull (we define ΔE as a measure of energy above the convex hull), as must all known high temperature, high pressure and metastable phases. Agreement is good but not perfect. We now address the disagreements.

The low and high temperature CaCd2 phases are reversed in energy relative to the experimental report that oI12 is stable at high temperatures and hP12 at low. The 11.6 meV/atom energy difference seems too large to be a flaw in our methods. However, the transition between the hP12 and oI12 variants has not been well established experimentally. Most likely, according to our findings, the presumed low temperature hP12 phase is actually a metastable phase, and the nominal high temperature phase is actually stable all the way to low temperatures.

The other disagreement is our finding that $Cd_{11}Ce$.cP36 touches the convex hull, predicting it should occur as a stable phase. This structure has not been reported in Ca-Cd. We find it to be marginally stable, lying 4.6 meV/atom below the line from CaCd6 to pure Cd, so small errors in our calculations could cause us to mis-predict stability. Alternatively, it may be truly stable but difficult to nucleate and grow.

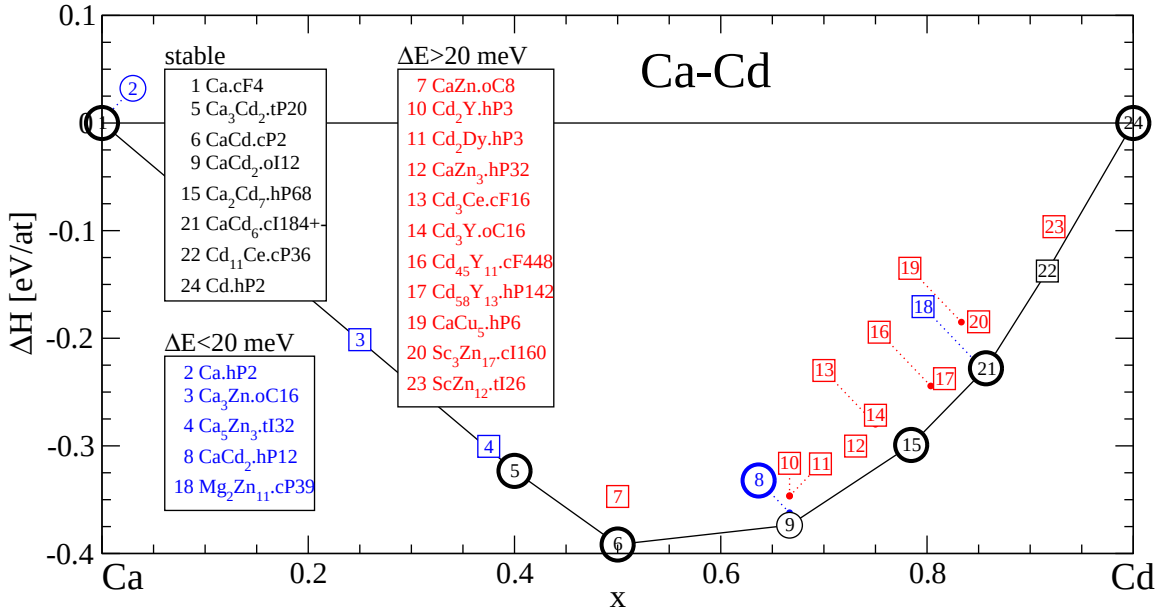

FIG. 3: Enthalpies of formation of Ca-Cd compounds. Notation: heavy circles indicate known low temperature phases; light circles indicate known high temperature phases; squares indicate either structures not reported in Ca-Cd system. Line segments connect vertices of convex hull. Legends list calculated stable structures ($\Delta E \equiv 0$), low but positve energy structures ($0 < \Delta E < 20$), and higher energy structures ($20 < \Delta E$). Additional data and structure details are available on the WWW [23]

IV. CCT DECORATION REFINEMENT AND NEW STRUCTURES

Given a specific tiling structure, modelling the i-CaCd atomic structure naturally breaks into two parts: (1) refining the decoration of glue atoms outside the clusters; (2) determining the optimal cluster center tetrahedron orientations.

We approach task (1) by comparison with known approximant structures (this fixes the decoration of the A, B and C cells) and by varying atomic decorations of the D tiling and optimizing their ab-initio energies. To build the initial starting model for the D-cell glue motif, we notice the apparent though surprising analogy between the Ca-Cd and α-AlMnSi decoration [24] with Ca on Mn sites and Cd on Al sites (strangely this interchanges the roles of large and small atoms) except for the following details: (i) The innermost two shells $s1$ and $s2$ of the basic Ca-Cd cluster replace the innermost icosahedron of the Al-Mn Mackay cluster; (ii) restore full SI order (from FCI in α-AlMnSi) by placing Cd on the "δ" sites (these sites are associated with body–center motifs of the 6D cubic hyperstructure) in all RD's, not just the even ones.

Extension of the α-AlMnSi structure to the CCT model has been studied in detail in Ref. [25]. We find that the glue atoms in both 1/1 and 2/1 approximants are entirely consistent with "dense SI" variant of the CCT i-AlMn model, and we have checked by calculating some 10 variant decorations of the D–cell model that our initial guess was energetically the most plausible one. In summary, our decoration rule allocates glue atoms as follows: (i) 2 Cd atoms with each CCT b-bond; (ii) 2 Cd atoms with each A-cell; (iii) 1 Ca and 1 Cd with each Y face; 6 Cd atoms with each Z–face; (iv) 3 Ca and 7 Cd atoms with each D cell. The precise assignement of these atoms will be described elsewhere. All model structures are available from [23].

Task 2 remains incomplete at the present time. We made some initial efforts by Monte Carlo annealing using a toy Ca-Cd pair potential to distribute Cd atoms among a list of possible sites based on experimental observations [4]. Unfortunately, this approach does not incorporate interactions of $s1$ tetrahedra in neighbouring clusters via distortion of the second shell ($s2$, Cd_{20} dodecahedron)) of the clusters. Indeed, Cd atoms from the tetrahedra can traverse from one cluster to another by pushing $s2$ atoms out of their nominal positions into "cube-center" positions [4] located on the 3-fold linkage between neighbouring clusters. These sites may serve either as a low-energy transient state for a Cd, and indeed such sites have non-zero occupancy in the 2/1 approximant.

ΔE values of our optimal decorations, listed for the tilings in table I, vary from +2 to +7 meV/atom. We attribute most of the energy variation to the problem of cluster center tetrahedron orientations. However, in the case of larger approximants incomplete k-point convergence and structural relaxation may also contribute. In cases of very large structures, we carried out some pre-relaxation using EAM potentials [22], because the ab-initio calculations were time- and memory-consuming.

V. DISCUSSION

We choose to model the Ca-Cd quasicrystal structure using real three-dimensional space rather than the six-dimensional space that is commonly used for quasiperiodic icosahedral structures. One reason for doing so is that many sites cannot be conveniently represented in the six-dimensional space, so the atomic surface structure would have to be quite complicated. Additionally, our calculation of energetics demands a focus on real space structure, especially because the smaller approximants that are in reach of first-principles calculation do not sample perpendicular space extensively. Yet, they provide all the variety needed to resolve tile decoration rules in real space.

Our final model yields a deterministic assignment of glue atoms within canonical cells. The cluster center tetrahedra are not deterministic, and follow as-yet undiscovered context-dependent rules. We have checked that the EAM Ca-Cd potentials describe accurately Ca-Cd energetics around the composition of interest. Resolving interesting questions regarding ordering of the tetrahedra inside the cluster motifs requires study of supercell models with large numbers of atoms, and appears to be beyond the reach within ab–initio calculational approach. However, this task may be doable using the EAM potentials.

Acknowledgments

This work was supported in part by NSF grant DMR-0111198. We thank Veit Elser for his IQtools program used to create figure 2, and we thank P. Brommer and F. Gähler for use of their EAM potentials. M. M. also acknowledges support from grants No. VEGA-2/5096/25, APVT-51021102, APVT-51052702 and SO-51/03R80603. Ab–initio calculations for largest approximant structures (ABC and ABCD series) were carried out under EC-funded project HPC-Europa, contract number 506079.

[1] A. P. Tsai, J. Q. Guo, E. Abe, H. Takakura, and T. J. Sato, Nature **408**, 537 (2000).
[2] J. Q. Guo, E. Abe, and A. P. Tsai, Phys. Rev. B **62**, R14605 (2000).
[3] J. Z. Jiang, C. H. Jensen, A. R. Rasmussen, and L. Gerward, Appl. Phys. Lett. **78**, 1856 (2001).
[4] C. P. Gomez and S. Lidin, Phys. Rev. B **68**, 024203 (2003).
[5] C. L. Henley, Phys. Rev. B **43**, 993 (1991).
[6] R. G. Hennig, A. E. Carlsson, K. F. Kelton, and C. L. Henley, Phys. Rev. B **71**, 144103 (2005).
[7] A. Palenzona, J. Less-Common Metals **25**, 367 (1971).
[8] G. Bruzzone, G. Chim. Ital. **102**, 234 (1972).
[9] H. Takakura, J. Guo, and A. P. Tsai, Phil. Mag. Lett. **81**, 411 (2001).
[10] Y. Ishii and T. Fujiwara, Phys. Rev. Lett. **87**, 206408 (2001).
[11] R. Tamura et al., J. Non-Cryst. Solids **334/335** (2004).
[12] R. Tamura, Y. Murao, S. Takeuchi, et al., Jpn. J. Appl. Phys. **41**, L524 (2002).
[13] R. Tamura, K. Edagawa, C. Aoki, S. Takeuchi, and K. Suzuki, Phys. Rev. B (2003).
[14] M. Widom and M. Mihalkovič (Mat. REs. Soc., 2004).
[15] C. P. Gomez and S. Lidin, Ang. Chem. Int. Ed. **40**, 4037 (2001).
[16] G. Kresse and J. Hafner, Phys. Rev. B **47**, RC558 (1993), Kresse and Furthmuller [17].
[17] G. Kresse and J. Furthmuller, Phys. Rev. B **54**, 11169 (1996).
[18] D. Vanderbilt, Phys. Rev. B **41**, 7892 (1990).
[19] G. Kresse and J. Hafner, J. Phys. Condens. Matter **6**, 8245 (1994).
[20] G. Kresse and J. Joubert, Phys. Rev. B **59**, 1758 (1999).
[21] e. a. T.B. Massalski, ed., *Binary Alloy Phase Diagrams* (ASM International, Materials Park, Ohio, 1990).
[22] Brommer and Gähler, in *Proceedings of ICQ9* (2005).
[23] Structure and energy data is available on the WWW at http://al loy.phys.cmu.edu.
[24] V. Elser and C. Henley, Phys. Rev. Lett. **55**, 2883 (1985).
[25] M. Mihalkovic, W. J. Zhu, C. L. Henley, et al. (????).